Evaluation of Radiolabeling PSMA-Targeted Long Circulating Peptide as a Theranostic Agent in Human Prostate Tumor-Bearing Mice

Ming-Hsin Li, Ming-Wei Chen, Wei-Lin Lo, Yuan-Ruei Huang, Sheng-Nan Lo, Shih-Ying Lee, Su-Jung Chen, Shih-Wei Lo, Shih-Min Wang, and Chih-Hsien Chang

1 Introduction

Prostate-specific membrane antigen (PSMA) is expressed higher in prostate tumors and metastases than most normal tissue. This pathological expression pattern leads it to be a target for endoradiotherapy of prostate cancer [1, 2]. The albumin binding structure has modified to the target molecule lets the kinetic of the molecule in the blood to change. In addition, extending the circulating-time of drugs in the body is a method to enhance the efficacy of drugs [3].

In this study, we have developed a novel long-circulation PSMA-targeted molecule, MH-PC-AB-56, which PSMA binding motif (PSMA-617 structure without DOTA) covalently linked with albumin binder (4-p-tolylbutyric acid), and conjugated DOTA chelator, and labeled with radionuclide ^{111}In or ^{177}Lu. We investigated the tumor binding affinity and biodistribution by molecular imaging of radiolabeled MH-PC-AB-56 peptide. The major objective of this study was to evaluate the potential advantage of MH-PC-AB-56 in the theranostic application by NanoSPECT image.

M.-H. Li (✉) · M.-W. Chen · W.-L. Lo · Y.-R. Huang · S.-N. Lo · S.-Y. Lee · S.-J. Chen · S.-W. Lo · S.-M. Wang · C.-H. Chang
Isotope Application Division, Institute of Nuclear Energy Research, Taoyuan, Taiwan
e-mail: mhli@iner.gov.tw

C.-H. Chang
e-mail: chchang@iner.gov.tw

K.-P. Lin et al. (eds.), *Future Trends and Challenges of Molecular Imaging and AI Innovation*, Springer Proceedings in Physics 272,
https://doi.org/10.1007/978-3-030-92786-8_11

2 Materials and Methods

A. Cell culture and tumor-bearing mice

The PSMA positive prostate cancer cell line, LNCaP, was obtained from Bioresource Collection and Research Center. Cells were grown in RPMI 1640 supplemented with 10% (v/v) fetal bovine serum, 100 units/mL penicillin and 100 μg/mL streptomycin in a humidified incubator at 37 °C under 5% CO_2. Six-week-old male BALB/c nude mice were obtained from BioLASCO Taiwan Co., Ltd. Mice were housed in a 12 h light cycle at 22 °C, with food and water provided ad libitum. Cells (1×10^7) was implanted right front leg of BALB/c nude mice for LNCaP tumor xenografts. The mice underwent NanoSPECT/CT study when the tumor volume reached approximately 200–600 mm^3. The animal experimental protocols were approved by INER Institutional Animal Care and Use Committee.

B. Radiolabeling with indium-111 and lutetium-177

Indium (^{111}In) chloride in 0.01 N HCl was generated from INER (Taoyuan, Taiwan). Lutetium (^{177}Lu) chloride in 0.04 N HCl purchased from ITM Medical Isotopes GmbH (Garching/Munich, Germany). The peptide (MH-PC-AB-56 and PSMA-617) purchased from Ontores Biotechnologies Co., Ltd. (Zhejiang China).

For ^{111}In-MH-PC-AB-56 labeling, the 13.9 nmole peptide (in DMSO) was incubation with 0.23–0.26 GBq $^{111}InCl_3$ in 1 M sodium acetate solution (pH 6.0) at 95°C for 15 min. The radiochemical efficiency analyzed by thin-layer chromatography (TLC) with 10% methanol and high-performance liquid chromatography (HPLC). For ^{177}Lu-MH-PC-AB-56 labeling, the 13.9 nmole peptide (in DMSO) was incubation with 0.47–0.51 GBq $^{177}LuCl_3$ in 0.4 M sodium acetate solution (pH 5.0) at 95°C for 30 min. The radiochemical efficiency analyzed by TLC with 0.1 M citric acid and HPLC. For ^{177}Lu-PSMA-617 labeling, the 19.2 nmole peptide (in water) was incubation with 0.47–0.51 GBq $^{177}LuCl_3$ in 0.4 M sodium acetate solution (pH 5.0) at 95°C for 30 min. The radiochemical efficiency analyzed by TLC with 0.1 M citric acid and HPLC. The specific activity for ^{111}In-MH-PC-AB-56, ^{177}Lu-MH-PC-AB-56 and ^{177}Lu-PSMA-617 in the range of 16.5–18.7 GBq/μmole, 33.8–36.7 GBq/μmole and 24.5–26.6 GBq/μmole, respectively.

The radiolabeled peptides were measured using a radioactive scanner (AR-2000 radio-TLC Imaging Scanner, Bioscan, France) and radio-HPLC with UV detector (280 nm) and radio detector. The column was waters T3 C18 column (3.5 μm, 80 Å, 4.6 × 250 mm). The flow rate was 0.8 mL/min with the gradient mobile phase going from 80% A buffer (0.1% TFA in water) and 20% B buffer (0.1% TFA in acetonitrile) to 90% B buffer within 10 min for ^{111}In-MH-PC-AB-56. The flow rate was 1.0 mL/min with the gradient mobile phase going from 95% A buffer (0.1% TFA in water) and 5% B buffer (0.1% TFA in acetonitrile) to 95% B buffer within 10 min for ^{177}Lu-MH-PC-AB-56. The flow rate was 1.0 mL/min with the gradient mobile phase going from 80% A buffer (0.1% TFA in water) and 20% B buffer (0.1% TFA in acetonitrile) to 60% B buffer within 10 min for ^{177}Lu-PSMA-617.

C. In vitro stability study

The stability of ^{111}In-MH-PC-AB-56 evaluated by incubation with normal saline (volume ratio 1:1) at room temperature or human serum (volume ratio 1:19) at 37°C [4]. The radiochemical purity determined by TLC and HPLC analysis at desired times (0, 1, 4, 24, 48, 72 and 96 h). The serum sample was prepared with acetonitrile/water solution and centrifuged at 13,000 rpm 2 min, then analyzed the supernatant by HPLC.

The stability of ^{177}Lu-MH-PC-AB-56 evaluated by incubation with normal saline (volume ratio 1:1) at room temperature. The radiochemical purity determined by HPLC analysis at desired times (0, 1, 2, 3, 4, 5, 6, 7, 8 and 24 h).

D. NanoSPECT/CT imaging

The procedure for NanoSPECT/CT imaging has been described, previously [5]. NanoSPECT and X-ray images were acquired using a NanoSPECT/CT plus scanner system (Mediso Medical Imaging Systems; Budapest, Hungary). The mice was anesthetized with 1–2% isoflurane during the imaging acquisition. NanoSPECT imaging was acquired using nine multipinholes gamma-detectors and high-resolution collimators. The energy window was set at 171 and 245 keV ± 10%, the image size was set at 256 ± 256, and the field of view of 60 mm × 100 mm. Each mouse was tail-vein injected with 19.4–20.7 MBq of radiolabeled peptide and scanned for 1 h, 4 h, 24 h, 48 h, 72 h and 96 h.

For calculating uptake value at an interesting organ of ^{111}In-MH-PC-AB-56 and ^{177}Lu-MH-PC-AB-56, the images of SPECT reconstructed by HiSPECT NG software (Scivis GmbH, Germany) and fused with CT datasets using InVivoScope software (Bioscan Inc.). Then, all data processed by PMOD Version 3.3 (PMOD Technologies Ltd., Zurich, Switzerland). Volumes of Interest (VOIs) drawn encompassing the tumor and reference source on the corresponding CT images. The VOIs transferred to SPECT images, and the count values of the tumor and reference source derived. The radioactivity of reference sources were 0.8 MBq ^{111}In and 1.3 MBq ^{177}Lu.

E. Statistics

Results presented as mean and standard deviation (Mean ± SD). The distribution correlation between ^{111}In-MH-PC-AB-56 and ^{177}Lu-MH-PC-AB-56 was analyzed by Pearson correlation coefficient (r) using IBM® SPSS® Statistics software version 19 [5].

3 Results

A. Radiolabeling efficiency of MH-PC-AB-56

The labeling efficiency of ^{111}In-MH-PC-AB-56 was 98.27 ± 1.29% and 99.09 ± 0.38% by TLC and HPLC analysis, respectively. In TLC, free ^{111}In was at origin front (Rf. approximately 0.000) and ^{111}In-MH-PC-AB-56 was at solvent front (Rf.

approximately 0.917) with 10% methanol as running buffer. The retention time of ^{111}In-MH-PC-AB-56 was 8.569 ± 0.010 min in radio detector by HPLC.

The labeling efficiency of ^{177}Lu-MH-PC-AB-56 was over 99.99% and 98.87 ± 0.73% by TLC and HPLC analysis, respectively. In TLC, free ^{177}Lu was at origin front (Rf. approximately 1.023) and ^{177}Lu-MH-PC-AB-56 was at solvent front (Rf. approximately 0.015) with 0.1 M citric acid as running buffer. The retention time of ^{177}Lu-MH-PC-AB-56 was 8.587 ± 0.262 min in radio detector by HPLC.

The labeling efficiency of ^{177}Lu-PSMA-617 was over 99.99% and 98.68% by TLC and HPLC analysis, respectively. In TLC, free ^{177}Lu was at solvent front (Rf. approximately 1.045) and ^{177}Lu-PSMA-617 had Rf. 0.435 with 0.1 M citric acid as eluted buffer. The retention time of ^{177}Lu-PSMA-617 was 8.247 min in radio detector HPLC.

B. In vitro stability study of ^{111}In-MH-PC-AB-56

The radio-purity of ^{111}In-MH-PC-AB-56 was greater than 95% within 96 h incubation in normal saline or human serum (Table 1).

C. In vitro stability of ^{177}Lu-MH-PC-AB-56 in normal saline

The stability of ^{177}Lu-MH-PC-AB-56 in normal saline was greater than 95% within 8 h incubation by HPLC (Table 2).

D. NanoSPECT/CT imaging

The images showed that both radiolabeled ^{111}In/^{177}Lu-MH-PC-AB-56 and ^{177}Lu-PSMA-617 were excreted mainly via the renal pathway with higher renal retention especially at early time points 1 h and 4 h injection. Higher and sustained tumor uptake was observed for radiolabeled MH-PC-AB-56 up to 96 h by imaging (Fig. 1).

The accumulated activity of radiolabeled ^{111}In/^{177}Lu-MH-PC-AB-56 in the tumor at time points was calculated from the images created by drawing the Volume of

Table 1 In vitro stability of ^{111}In-MH-PC-AB-56 at different times after incubation in normal saline at room temperature or human serum at 37°C

Time (h)	Normal Saline		Human Serum	
	TLC (%)	HPLC (%)	TLC (%)	HPLC (%)
0	99.5 ± 0.9	98.8 ± 1.1	98.3 ± 0.8	98.8 ± 0.3
1	98.6 ± 1.3	97.9 ± 1.2	98.2 ± 0.9	98.9 ± 0.6
4	98.7 ± 1.2	97.0 ± 0.8	98.8 ± 1.1	99.2 ± 0.1
24	99.2 ± 0.7	97.8 ± 0.8	98.0 ± 1.0	99.0 ± 0.4
48	99.6 ± 0.8	97.4 ± 1.1	98.3 ± 0.6	99.0 ± 0.3
72	99.0 ± 0.8	96.6 ± 0.7	98.1 ± 0.5	98.7 ± 0.6
96	96.9 ± 2.8	98.5 ± 0.9	95.5 ± 0.8	98.8 ± 0.3

(mean ± SD, n = 3)

Table 2 In vitro stability of ^{177}Lu-MH-PC-AB-56 at different times after incubation in normal saline at room temperature (mean ± SD, n = 3)

Time (h)	Normal Saline HPLC (%)
0	99.5 ± 0.6
1	98.0 ± 0.9
2	96.6 ± 2.7
3	96.9 ± 1.0
4	94.5 ± 2.5
5	96.2 ± 1.4
6	94.9 ± 1.8
7	94.3 ± 1.1
8	94.4 ± 1.2

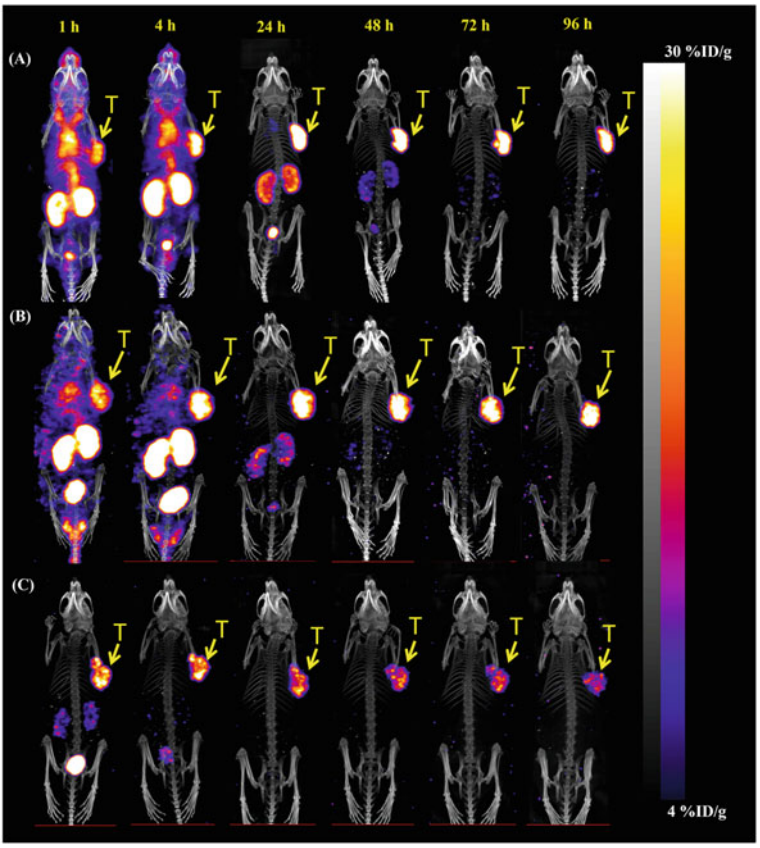

Fig.1 Comparison of NanoSPECT/CT images of ^{111}In-MH-PC-AB-56 (**a**), ^{177}Lu-MH-PC-AB-56 (**b**) or ^{177}Lu-PSMA-617 (**c**) targeting LNCaP tumor-bearing mice. The images were acquired at 1, 4, 24, 48, 72, and 96 h after injection

Table 3 Comparison of tumor uptake of ^{111}In-MH-PC-AB-56 and ^{177}Lu-MH-PC-AB-56 analyzed by NanoSPECT image

Time (h)	^{111}In-MH-PC-AB-56 (%ID/g)	^{177}Lu-MH-PC-AB-56 (%ID/g)
1	19.79 ± 2.27	12.91 ± 2.69
4	27.32 ± 2.85	17.98 ± 3.20
24	43.79 ± 6.55	22.08 ± 6.63
48	35.48 ± 4.53	21.56 ± 4.90
72	29.77 ± 4.30	22.80 ± 5.29
96	25.06 ± 3.77	23.41 ± 5.18

Interest (VOI) using the standard source as a point of reference. The image semi-quantitative analysis of ^{111}In-MH-PC-AB-56 in the tumor at 1 h, 4 h, 24 h, 48 h, 72 h and 96 h after injection was 19.79 ± 2.27, 27.32 ± 2.85, 43.79 ± 6.55, 35.48 ± 4.53, 27.77 ± 4.30, and 25.06 ± 3.77%ID/g, respectively (Table 3). The image semi-quantitative analysis of ^{177}Lu-MH-PC-AB-56 in the tumor at 1 h, 4 h, 24 h, 48 h, 72 h and 96 h after injection was 12.91 ± 2.69, 17.98 ± 3.20, 22.08 ± 6.63, 21.56 ± 4.90, 22.80 ± 5.29, and 23.41 ± 5.18%ID/g, respectively (Table 3). The trend of tumor uptake of ^{111}In-MH-PC-AB-56 is similar to ^{177}Lu-MH-PC-AB-56 before 24 h injection. After 24 h injection, the tumor uptake of ^{111}In-MH-PC-AB-56 was slightly declining, but the tumor uptake of ^{177}Lu-MH-PC-AB-56 sustained last for at least 96 h.

Pearson correlation analysis of tumor uptake of ^{111}In-MH-PC-AB-56 and ^{177}Lu-MH-PC-AB-56 by semi-quantification image analysis was moderated degree ($r = 0.576$). There was a high correlation of liver, kidney, and muscle of ^{111}In-MH-PC-AB-56 and ^{177}Lu-MH-PC-AB-56 with value 0.960 (Table 4), 0.960 (Table 5), and 0.940 (Table 6), respectively.

Table 4 Comparison of liver accumulation of ^{111}In-MH-PC-AB-56 and ^{177}Lu-MH-PC-AB-56 analyzed by NanoSPECT image (mean ± SD, n = 3)

Time (h)	^{111}In-MH-PC-AB-5 (%ID/g)	^{177}Lu-MH-PC-AB-56 (%ID/g)
1	9.89 ± 2.25	4.38 ± 1.22
4	8.31 ± 2.10	2.33 ± 0.51
24	1.84 ± 0.47	0.36 ± 0.11
48	0.53 ± 0.20	0.25 ± 0.09
72	0.32 ± 0.16	0.17 ± 0.05
96	0.23 ± 0.10	0.19 ± 0.02

Table 5 Comparison of kidney accumulation of ^{111}In-MH-PC-AB-56 and ^{177}Lu-MH-PC-AB-56 analyzed by NanoSPECT image (mean ± SD, n = 3)

Time (h)	^{111}In-MH-PC-AB-56 (%ID/g)	^{177}Lu-MH-PC-AB-56 (%ID/g)
1	37.62 ± 3.69	40.35 ± 4.89
4	39.66 ± 7.59	42.63 ± 20.14
24	16.40 ± 3.82	6.33 ± 3.51
48	6.15 ± 1.39	2.46 ± 1.39
72	3.19 ± 0.75	1.57 ± 0.95
96	2.02 ± 0.74	0.92 ± 0.68

Table 6 Comparison of muscle accumulation of ^{111}In-MH-PC-AB-56 and ^{177}Lu-MH-PC-AB-56 analyzed by NanoSPECT image (mean ± SD, n = 3)

Time (h)	^{111}In-MH-PC-AB-56 (%ID/g)	^{177}Lu-MH-PC-AB-56 (%ID/g)
1	6.58 ± 0.59	3.76 ± 1.15
4	6.70 ± 0.45	2.22 ± 0.84
24	1.29 ± 0.27	0.43 ± 0.23
48	0.41 ± 0.06	0.25 ± 0.07
72	0.21 ± 0.05	0.18 ± 0.07
96	0.17 ± 0.01	0.18 ± 0.01

4 Conclusions and Discussion

Many albumin binders (truncated Evan's blue, 4-(phenyl)butyric acid, 4-(p-bromophenyl)butyric acid, 4-(p-iodophenyl)butyric acid, 4-(p-chlorophenyl)butyric acid, 4-(p-fluorophenyl)butyric acid, 4-(p-methyl phenyl)butyric acid, and 4-(p-methoxyphenyl)butyric acid) had been used in modified PSMA-617 to enhance the circulating-time of PSMA-targeted drug to drawdown the accumulation of drug at kidney and improved tumor uptake [6]. We explored a novel linker lysine and 6-aminohexanoic acid not like PSMA-ALB-56 [7] only lysine or RPS [8] used PEG before. The structure is not only longer of length than lysine but also more lipophilic than PEG. In vitro stability study showed, the radiochemical purity of ^{177}Lu-MH-PC-AB-56 maintain to over 90% last at least 8 h without ascorbic acid addition. The SPECT image show that MH-PC-AB-56 labeled with dual-nuclide have a similar trend of metabolism or elimination organ, and demonstrated ^{177}Lu-MH-PC-AB-56 could improve tumor uptake than 177Lu-PSMA-617. These results let us know the tumor accumulated ability and elimination route of radiolabeled MH-PC-AB-56. These results indicated the ^{111}In/^{177}Lu-MH-PC-AB-56 owned the theranostic potency for diagnosis and therapy. The therapeutic efficacy, pharmacokinetics, and biodistribution would be further studied in the near future.

Acknowledgements We thanked the support from the Ministry of Economic Affairs, ROC with grant number 108-EC-17-A-22-1587.

Conflict of Interest The authors declare that they have no conflict of interest.

References

1. Rahbar et al (2018) Mol Imaging 17:1–9. https://doi.org/10.1177/1536012118776068
2. Langbein et al (2019) J Nucl Med 60:13S-19S. https://doi.org/10.2967/jnumed.118.220566
3. Kuo et al (2018) Mol Pharmaceutics 15:5183–5191. https://doi.org/10.1021/acs.molpharmaceut.8b00720
4. Lo et al (2020) Appl Radiat Isot 161:109126. https://doi.org/10.1016/j.apradiso.2020.109162
5. Chang et al (2007) Anticancer Res 27:2217–2226
6. Kuo et al (2020). J Nucl Med. https://doi.org/10.2967/jnumed.120.250738
7. Umbricht et al (2018) Mol Pharm 15:2297–2306. https://doi.org/10.1021/acs.molpharmaceut.8b00152
8. Kelly et al (2019) J Nucl Med 65:656–663. https://doi.org/10.2967/jnumed.118.221150